

SURFACE CHARACTERIZATION AND FIELD EMISSION MEASUREMENTS OF COPPER SAMPLES INSIDE A SCANNING ELECTRON MICROSCOPE

J. Ögren *, S. H. M. Jafri, K. Leifer, V. Ziemann, Uppsala University, Uppsala, Sweden

Abstract

Vacuum breakdown in normal-conducting accelerating structures is a limiting factor for high gradient acceleration. Many aspects of the physics governing the breakdown process and its onset are yet to be fully understood. At Uppsala University we address these questions with an in-situ experimental setup mounted in an environmental scanning electron microscope. It consists of a piezo motor driven tungsten needle and a sample surface mounted on a piezo stage, allowing for nano-meter 3D-position control. One of the piezo motors controls the needle-sample gap while the two other scan across the surface. A DC-voltage up to 1 kV is applied across the gap and field emission currents from a copper surface are measured with an electrometer. Here we present the setup and some initial results.

INTRODUCTION

The performance and efficiency of future linear accelerators for high energy physics [1] is determined by the quality of the radio-frequency structures used to accelerate the particle beams. The high electromagnetic field levels required to keep the accelerator compact, cause field emission and occasional spontaneous discharges or breakdown of the radio-frequency fields [2] on the inner surfaces of the structures. In super-conducting structures the surface morphology and chemistry proved to be decisive features that were improved [3] over the past 30 years and led to a hugely increased achievable gradients. Normal-conducting structures have reached a stage where the high design gradients are reached [4], albeit with breakdown levels that are marginal. Since the breakdown events are determined by the surface physics on the inner surfaces of the structures we have built a device that allows us to place a probe needle on high-voltage over a sample surface to locally study the pre-breakdown stage, subsequent breakdown and the final creation of craters inside a scanning electron microscope. The present scanner is an improved version of the one discussed in ref. [5].

FIELD EMISSION

The theory of field emission was first properly formulated by Fowler and Nordheim in 1928 [6]. They derived an equation for current density as function of electric field. The equation for field emission was improved to include temperature effects [7]. We use a form commonly used [8, 9] for

field emission

$$I = A_e \frac{1.54 \times 10^6 \beta^2 E^2}{\phi} e^{10.41\phi^{-1/2}} \times e^{-6.53 \times 10^3 \phi^{3/2} / \beta E} \tag{1}$$

This can be written in the form of

$$\ln \left\{ \frac{I}{E^2} \right\} = m - \frac{k}{E} \tag{2}$$

and if we plot $\ln \left\{ \frac{I}{E^2} \right\}$ versus $\frac{1}{E}$ we can determine the local field enhancement β from the slope of the curve. In our case we use copper samples of quality similar as used for the Compact Linear Collider (CLIC) accelerating structures. The value of the work function of copper $\phi = 4.5$ eV.

SYSTEM DESCRIPTION

The setup consists of a sample holder designed for circular samples with 12 mm diameter. The sample holder is mounted on piezo motors which allows position control in x - y direction. A tungsten needle is mounted on another piezo motor for controlling the gap distance. The SmarAct SLC1720 piezo motors all have position sensors with nanometer resolution and are controlled by a MCS-3C controller, which makes position control with nanometer precision possible. The setup with the piezo motors is shown in Fig. 1. A Keithley 6517A electrometer is used for sourcing voltage up to 1000V and simultaneously measuring currents with sub-pA resolution. A summary of the parameters is presented in Table 1.

Table 1: System Parameters

Parameter	value
Voltage source	0-1000V
Current measurement resolution	sub-pA
Position control	1 nm
Sample diameter	12 mm
Tungsten needle radius of curvature	5 μ m
Vacuum level in SEM	5×10^{-5} mBar

The setup can be placed inside the vacuum chamber of a scanning electron microscope (SEM), we use an environmental SEM Philips XL30 ESEM-FEG. This makes in-situ measurements of field emission currents and observation of small surface changes with high resolution possible. The setup is mounted on the sample holder of the SEM which can be moved in 5 degrees of freedom, this controls where, and with what angle, on the sample surface we probe the electron microscope. On top of this we have the degrees of freedom of our setup which controls where on the surface

* jim.ogren@physics.uu.se

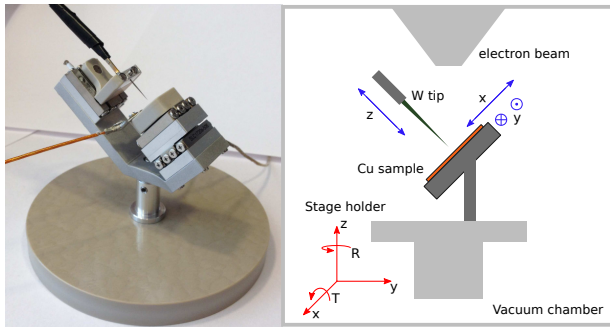


Figure 1: *Left*: The setup with piezo motors for controlling the x - y direction of the sample surface and gap distance between needle and surface. The bottom plate is only for holding the setup when not installed in the SEM. *Right*: A schematic of the setup inside the vacuum chamber of the SEM.

we perform the field emission measurements. With the last piezo motor we can control the gap distance. A schematic of the setup inside the SEM is shown in Fig. 1.

Knowing the gap distance between needle and surface is crucial in order to determine the macroscopic electric field. To determine the gap distance we apply a low voltage of 1 V across the gap and slowly approach the surface while monitoring the electric current. When the current exceeds a threshold the procedure stops. Typically we can move to a gap distance of about $5 \mu\text{m}$ just from the images from the electron microscope and then we start decreasing the gap distance further in steps of a few nanometers using the piezo motors. Repeated measurements showed good reproducibility and we performed a series of 10 measurements of the gap distance with only $\sigma = 20 \text{ nm}$ standard deviation. At present we have a tungsten needle with some rough features and the physical contact of the needle and the surface left marks on the surface. These dents may give rise to a systematic error in the measured gap distance. Since we do not want to make field emission measurements at a location where we have damaged the surface we can measure the gap distance at two surrounding points and interpolate between the two points. Then we move to a position in the middle of the two points and set a desired gap distance without physical contact between the surface and the needle.

PRELIMINARY RESULTS

We performed a series of 10 voltage scans at the same position with gap distance set to 500 nm. In the voltage scans we measured the current while ramping voltage in steps of 2 V until a threshold of $1 \mu\text{A}$ was reached. Figure 2 shows the maximum voltage, i.e. the voltage when the current threshold was reached. As can be seen the highest voltage was reached in the first scan and then maximum voltage decreased in the scans that followed. For each scan step we performed the same analysis and determined field enhancement factor β and as we can see in Fig. 2 there was a peak in field enhancement in scan step 7 leading to a

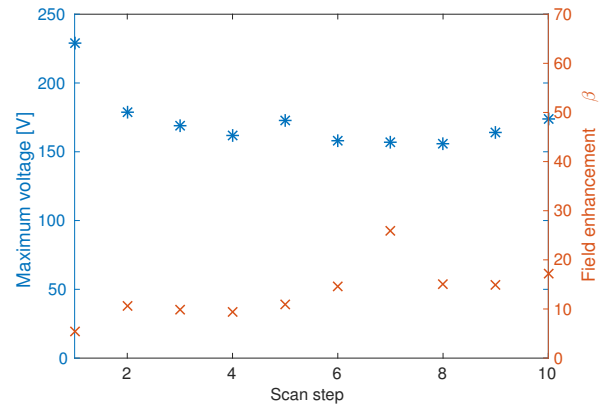


Figure 2: The maximum voltage and field enhancement for 10 voltage scans. A peak in field enhancement was reached at scan step 7.

maximum local electric field at this scan step. We note that the initial scan step reached the highest maximum voltage and the lowest field enhancement. The subsequent scans had lower voltage but higher field enhancement which gives the impression of an activation effect.

Scanning electron microscope images as shown in Fig. 3, before and after the scan, show the formation of crater with a diameter of $4 \mu\text{m}$ during the experiment. As we can observe from Fig. 3, the sample has low surface roughness. Furthermore, it can be observed that the enhanced field emission that leads to the formation of crater occurs in the flat regions of sample. Higher magnification image shows some 100 nm protrusions on the surface of the sample. The location of protrusions before and after the field emission is outside the region of crater, hence these protrusions have not played any part in the formation of the crater during field emission but was effected by the creation of crater itself.

In another experiment, we performed a series of 100 voltage scans at another location on the surface. Again we used gap distance 500 nm and the same settings as in the previous scan. Figure 4 shows the maximum voltage and field enhancement factor β . This time we could not observe any changes on the surface, i.e. no crater formation. However, around scan step 25 there was a sudden increase in maximum voltage. But there was simultaneously a decrease in field enhancement. This compensates the increase in voltage and thus keeping the maximum local electric field fairly constant. To quantify the steps we performed fits to both the maximum voltage and the field enhancement in the form

$$f(n) = a + \frac{b}{\pi} \arctan(n - c) \quad (3)$$

where n is the scan step number. The fit results are summarized in Table 2. As we can see there is a 62 V step in maximum voltage and -3 step in field enhancement between steps 25-26. This would suggest that one or several field emitters disappeared, e.g. melted, due to the intense surface electric field and high current density.

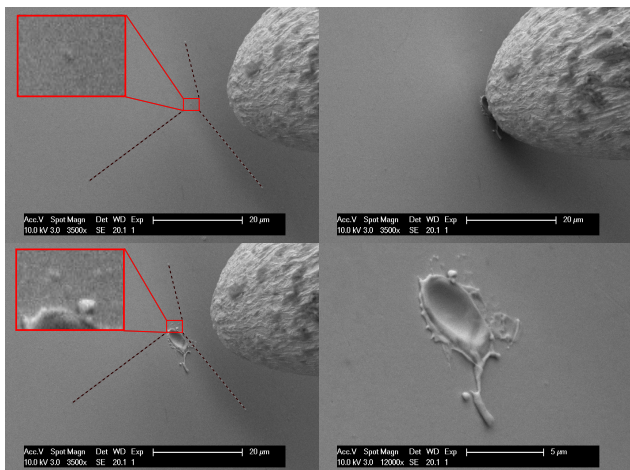


Figure 3: A crater formed during the series of 10 voltage scans. *Top left*: surface before measurement, to the right of the image we see the tip of the tungsten needle which was retracted 10 μm to not block the view of the surface. We also show a zoom of a small protrusion on the surface. *Top right*: needle at surface directly after measurement, crater was formed. *Bottom left*: surface after measurement. We used the dashed lines for triangulation to locate the small protrusion again. *Bottom right*: zoom in of the crater. The diameter of the crater is a few microns. We also note the smoothness of the surrounding surface.

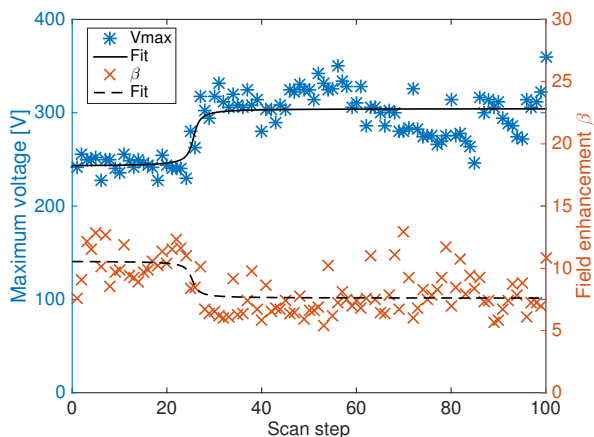


Figure 4: The maximum voltage applied and the field enhancement factor for 100 voltage scans. There is a sudden increase in maximum voltage and simultaneously a decrease in field enhancement.

Table 2: Fit Results Value (Confidence Limits)

	Vmax	β
<i>a</i>	273.5 (268.6, 278.4)	9.1 (8.7, 9.5)
<i>b</i>	62 (52, 72)	-3.0 (-3.8, -2.2)
<i>c</i>	25.6 (23.9, 27.3)	25.3 (22.6, 28.0)

In the series of 100 scans there was no clear peak in field enhancement and no crater was formed. We also note that the field enhancement factor was on average lower than compared to the series of 10 scans. We can only conjecture that the crater in the series of 10 scans was formed in step 7, when beta was largest, since we only observed the surface before and after the series.

In total we have performed many different voltage scans but only in a handful of the measurements did we observe visible damages on the surface and at locations without any special, visible surface features. This might suggest that the field enhancement and onset of breakdown might not be dependent on surface roughness but something else, perhaps surface chemistry.

CONCLUSION

We constructed a setup for in-situ SEM field emission measurements we nanometer-precision position control. The small dimensions of the setup and small size of the tungsten needle allows for field emission measurements localized to a small part of the surface. The benefit of in-situ SEM experiments is that we can easily observe the surface before and after the field emission measurements. We performed series of voltage scans with field emission and in some cases we saw crater formation. In the experiment with a crater formation it did not seem to be a correlation to surface morphology. This suggests that, for well-treated samples with flat surfaces, the field emission currents do not so much depend on surface morphology, but rather on something else such as surface chemistry.

REFERENCES

- [1] CLIC Conceptual Design Report, CERN Technical Report No. CERN-470 2012-007 (2012).
- [2] E. Tanabe, IEEE Trans. Nucl. Sci., NS-30 (1983) 3351.
- [3] A. Pandey, G. Muller, D. Reschke, and X. Singer, Phys. Rev. ST Accel. Beams 12 (2009) 023501.
- [4] R. Ruber, et al., The CTF3 Two-beam Test Stand, Nucl. Inst. and Methods A 729 (2013) 546.
- [5] T. Muranaka, T. Blom, K. Leifer, V. Ziemann, Instrumental developments for in situ breakdown experiments inside a scanning electron microscope, Nucl. Inst. and Methods A 657 (2011) 122.
- [6] R. H. Fowler and L. Nordheim, Proc. R. Soc. Lond. A 119 173 (1928).
- [7] E. L. Murphy and R. H. Good, Phys. Rev. 102, 1464 (1956).
- [8] J.W. Wang, G.A. Loew, SLAC-PUB-7684, 1997.
- [9] A. Grudiev, S. Calatroni and W. Wuensch, Phys. Rev. ST Accel. Beams 12, 102001 (2009)